JPL PUBLICATION 84-16

NASA-CR-173728
19840019646

Satellite Emission Range Inferred Earth Survey (SERIES) Project: Final Report on Research and Development Phase, 1979 to 1983

L.A. Buennagel
P.F. MacDoran
R.E. Neilan
D.J. Spitzmesser
L.E. Young

March 1, 1984

NASA
National Aeronautics and
Space Administration

Jet Propulsion Laboratory
California Institute of Technology
Pasadena, California

```
     EXPAND     RN/ JPL-84-16
     MISSING OR INVALID OPERAND IN YOUR COMMAND
================================================================================
 25      1      1 RN/JPL-PUB-84-16
           DISPLAY 25/2/1
       84N27714*#   ISSUE 18   PAGE 2791   CATEGORY 4   RPT#: NASA-CR-173728
       JPL-PUB-84-16 NAS 1.26:173728   CNT#: NAS7-918   84/03/01  54 PAGES
       UNCLASSIFIED DOCUMENT
UTTL:  Satellite Emission Range Inferred Earth Survey (SERIES) project   TLSP:
       Final Report, 1979 - 1983
AUTH:  A/BUENNAGEL, L. A.;  B/MACDORAN, P. F.;  C/NEILAN, R. E.;  D/SPITZMESSER,
       D. J.;  E/YOUNG, L. E.
CORP:  Jet Propulsion Lab., California Inst. of Tech., Pasadena.    AVAIL.NTIS
       SAP: HC A04/MF A01
MAJS:  /*GEODESY/*GLOBAL POSITIONING SYSTEM/*MICROWAVE FREQUENCIES/*NAVIGATION/*
       SPACECRAFT TRACKING
MINS:  / ACCURACY/ COST EFFECTIVENESS/ GUIDANCE (MOTION)/ RADIO STARS/ VERY LONG
       BASE INTERFEROMETRY
ABA:   Author
ABS:   The Global Positioning System (GPS) was developed by the Department of
       Defense primarily for navigation use by the United States Armed Forces.
       The system will consist of a constellation of 18 operational Navigation
       Satellite Timing and Ranging (NAVSTAR) satellites by the late 1980's.
       During the last four years, the Satellite Emission Range Inferred Earth
       Surveying (SERIES) team at the Jet Propulsion Laboratory (JPL) has
       developed a novel receiver which is the heart of the SERIES geodetic
       system designed to use signals broadcast from the GPS. This receiver does
ENTER:
```

JPL PUBLICATION 84-16

Satellite Emission Range Inferred Earth Survey (SERIES) Project: Final Report on Research and Development Phase, 1979 to 1983

L.A. Buennagel
P.F. MacDoran
R.E. Neilan
D.J. Spitzmesser
L.E. Young

March 1, 1984

National Aeronautics and
Space Administration

Jet Propulsion Laboratory
California Institute of Technology
Pasadena, California

The research described in this publication was carried out by the Jet Propulsion Laboratory, California Institute of Technology, under a contract with the National Aeronautics and Space Administration.

PREFACE

The work described in this report is a consequence of many years of research and development activity on the use of radio interferometry at microwave frequencies using compact radio stars as the sources of radio signals. The initial SERIES engineering configuration, using the NAVSTAR satellites instead of quasars, was to process the data by the Very Long Baseline Interferometry (VLBI) techniques. This approach resulted in a complexity of data processing which was not compatible with the concept of using the much stronger radio signals. Fortunately, it turned out that using the one-way range measurement from the satellite to each of the two earth stations greatly simplified the entire project. Although the primary dedication of the research was to create a system competitive in accuracy with the VLBI and laser ranging techniques (but at much less cost in capital expenditures), two additional significant results were achieved: 1) the ability to synchronize clocks to the few nanosecond level at intercontinental distances in near real time, and 2) the ability to measure the total columnar content of free electrons between the NAVSTAR satellite and the earth receiver along the line of sight between them.

N. A. Renzetti, Manager
JPL Geodynamics Program

ACKNOWLEDGEMENT

The authors wish to acknowledge the support of Mr. T. L. Fischetti of NASA Headquarters for his foresight in funding the feasibility and proof-of-concept work at JPL with regard to the application of the Global Positioning System for precision earth surveying.

The authors gratefully acknowledge the assistance of their JPL colleagues: M. G. Newsted, M. A. Smith and S. Harmon for the mechanical design and fabrication of the portable stations; J. B. Thomas for theoretical studies and system analysis; G. M. Resch and D. W. Curkendall for discussions on system design options; H. N. Royden, R. M. Miller, and T. E. Litwin for VHF Faraday rotation ionospheric monitoring at Goldstone, CA; A. L. Berkin for assistance in taking data; S. J. DiNardo and C. J. Vegos for logistical support. The cooperation of F. B. Varnum, Defense Mapping Agency and Sergeant Wagner, Vandenberg AFB, is also acknowledged for making available the approximate GPS satellite ephemerides used in the SERIES microcomputer for pointing the 1.5 m antennas.

CONTENTS

Figures

ABSTRACT

The Global Positioning System (GPS) was developed by the Department of Defense primarily for navigation use by the United States Armed Forces. The system will consist of a constellation of 18 operational Navigation Satellite Timing and Ranging (NAVSTAR) satellites by the late 1980's.

During the last four years, the Satellite Emission Range Inferred Earth Surveying (SERIES) team at the Jet Propulsion Laboratory (JPL) has developed a novel receiver which is the heart of the SERIES geodetic system designed to use signals broadcast from the GPS. This receiver does not require knowledge of the exact code sequence being transmitted. In addition, when two SERIES receivers are used differentially to determine a baseline, few cm accuracies can be obtained.

The initial engineering test phase has been completed for the SERIES Project. Baseline lengths, ranging from 150 meters to 171 kilometers, have been measured with 0.3 cm to 7 cm accuracies. This technology, which is sponsored by the NASA Geodynamics Program, has been developed at JPL to meet the challenge for high precision, cost-effective geodesy, and to complement the mobile Very Long Baseline Interferometry (VLBI) system for Earth surveying.

I. INTRODUCTION

The commonly accepted model of the structure of the Earth's crust is that it is composed of a set of tectonic plates. One of the stated objectives of the NASA Geodynamics Program is to contribute to the understanding of the processes that result in the movement and deformation of these tectonic plates. The average rates of interplate motion over geologic time scales have been determined from the geologic record to be in the range of a few centimeters per year, but whether this motion is constant or episodic is currently unknown.

Two space-based techniques, currently being supported by the Geodynamics program, have been developed, and are capable, in principle, of measuring the motions between plates in real time (a few years). These techniques are Very Long Baseline Interferometry (VLBI) and Satellite LASER Ranging (SLR).

In addition to the large scale movement between tectonic plates, more complicated motion in the Earth's crust is known to occur. An example of this would be the local crustal distortion caused by the strain accumulation and release near the boundaries of plates. It is necessary to describe such motion in detail in order to be able to deduce the physical processes at work, or to generalize such plate boundary interactions for study of the forces that drive and resist plate motion. In order to adequately characterize these distortions, it is necessary to measure a grid of reference points that is densely sampled in space and time.

It is not possible to make such measurements using VLBI or SLR techniques due to economic considerations. The requirement for the dense set of accurate geodetic measurements, needed for regional geodesy and a number of related studies, is the motivation for developing the Satellite Emission Range Inferred Earth Surveying (SERIES) Global Positioning System (GPS) receiver which is described in this report.

Two proof-of-concept SERIES stations (Fig. 1) have been constructed. These stations each have a 1.5-m diameter prime feed parabolic dish antenna

Figure 1. One of the two SERIES proof-of-concept stations. Data aquisition electronics occupy a small portion of the camper shell. The antenna is a 1.5 meter diameter, prime focus feed dish mounted on a two axis (azimuth and elevation) drive.

which provides approximately 23 dB of gain in the GPS signal. The receivers have been constructed from off-the-shelf components wherever possible (Ref. 1). The receivers contain a locally generated test signal for self-calibration. Data can be recorded on either floppy disks or 9-track tapes.

The original SERIES implementation was to use the NAVSTARs as Radio Frequency (RF) noise sources for Very Long Baseline Interferometry (VLBI) terminals (Ref. 2). However, it was realized that the periodic structure in the GPS signal could be used to provide ranging information even without code sequence knowledge. By exploiting the periodic structure, the GPS signal bandwidths were collapsed, and the data acquisition and post-processing were greatly simplified.

The proof-of-concept stations have been tested on baselines up to 171 km during the last year and a half. Baseline vectors determined with the SERIES stations have demonstrated few cm measurement accuracies for baselines of a few tens of km (Ref. 3).

These SERIES stations are also capable of measuring the total columnar content of free electrons integrated along the path between the receiver and the GPS satellite. This measurement was validated through comparison with a co-located Faraday rotation device, obtaining agreement to 10^{16} electrons per meter squared (Ref. 4).

An additional feature of the SERIES technique is the ability to synchronize clocks at different sites by receiving common signals from the satellite. This was demonstrated by comparisons of clock offsets measured with the SERIES stations against independent measurements made simultaneously with an atomic clock carried between the two stations (Ref. 5). The agreement between the two techniques was within 1 nanosecond (10^{-9} second) for each of the two experiments performed. The SERIES technique for clock synchronization is expected to give accuracies of 1 to 10 nanoseconds for intercontinental station separations.

Development of the SERIES technology is currently underway at JPL for the following applications:

1. High-precision, cost-effective Earth surveying

2. Precision orbit determination of low-Earth orbiters

3. The precise positioning of marine platforms to aid in the measurement of sea floor motions.

II. STATEMENT OF THE CHALLENGE

The satellite constellation of the GPS, when fully implemented in the late 1980's, will be composed of 18 Earth satellites (Ref. 6). This constellation will illuminate the Earth with dual L-band microwave signals intended to serve, primarily, U.S. military needs for positioning and navigation. At this writing, six satellites are in orbit and functional. The three main elements of the GPS are the satellite segment (termed NAVSTAR) which develops L-band signals from on-board atomic clocks and disseminates satellite ephemeris information; a ground control segment that monitors and controls the ephemeris of each satellite and the clocks in orbit; and a user segment that receives the L-band signals to accomplish a wide variety of positioning and navigation functions. Because of the nature of military missions, each segment of the GPS has capability which is restricted, and the highest precision NAVSTAR transmissions are encrypted in a manner originally designed to be unavailable to the public.

In its highest precision mode for point positioning of a single receiver, the GPS is required to have an accuracy of 16 meters in three dimensions. However, for certain applications, such as crustal deformation monitoring to provide inputs for geophysical modeling, sub-decimeter relative positioning accuracy is the threshold of interest. The challenge is to devise a system which (1) exploits the technology of the existing Global Positioning System; (2) operates sans knowledge of the codes, while simultaneously obtaining an accuracy level three orders of magnitude better than required by the original GPS design; and (3) achieves these results with inexpensive equipment and cost-effective data processing.

III. THEORY OF OPERATION

In order to understand the SERIES concept of GPS, it is useful to consider the convential mode of operation in which the user has access to the codes (see Fig. 2). Suppose an observer is located at a geocentric vector position described as $\vec{R}_u$ with the NAVSTAR-GPS located at geocentric vector position $\vec{\rho}_s$. The observer acquires the satellite broadcast when the satellite rises above the horizon. Imagine that the clock aboard the satellite, registering t_s, and the clock at the observer's radio receiver, registering t_u, are synchronized. If the apparent delay in the arrival of the satellite clock pulses is Δt, then the apparent range to the satellite is $\rho = c\,\Delta t$, where c is the speed of light.

The magnitude of the range varies between 25×10^6 meters at satellite rise and is set to a minimum of 20×10^6 meters at the Time of Closest Approach (TCA) to the observer's position. The rate of change of range causes the P-code modulation to vary from its true frequency (f = 10.23 MHz) by an amount equal to ±27 Hz with the true frequency value being observed at approximately TCA. However, in the real world, neither the user's nor the satellite's clock is exactly synchronized to an external frequency standard such as Universal Time Coordinated (UTC). This results in an error in the observed range. The observed range, ρ', now appears as

$$\rho' = \left| \vec{\rho}_s - \vec{R}_u \right| + c(\Delta t_u - \Delta t_s)$$

where the subscripts u and s denote user and satellite, respectively, and the Δt_u and Δt_s indicate clock bias with respect to the UTC. Also, the measured frequency of the satellite signals, f_m, is in error by a summation of errors in the clock rate of both user and satellite clocks, as well as errors due to atmospheric range rate terms. This type of GPS measurement is also known as single point or absolute positioning.

In the conventional GPS configuration, the terms $\vec{p}_s$ and Δt_s are supplied to the user by a 50 bit-per-second telemetry message which contains satellite ephemeris and clock state information. When a user decrypts

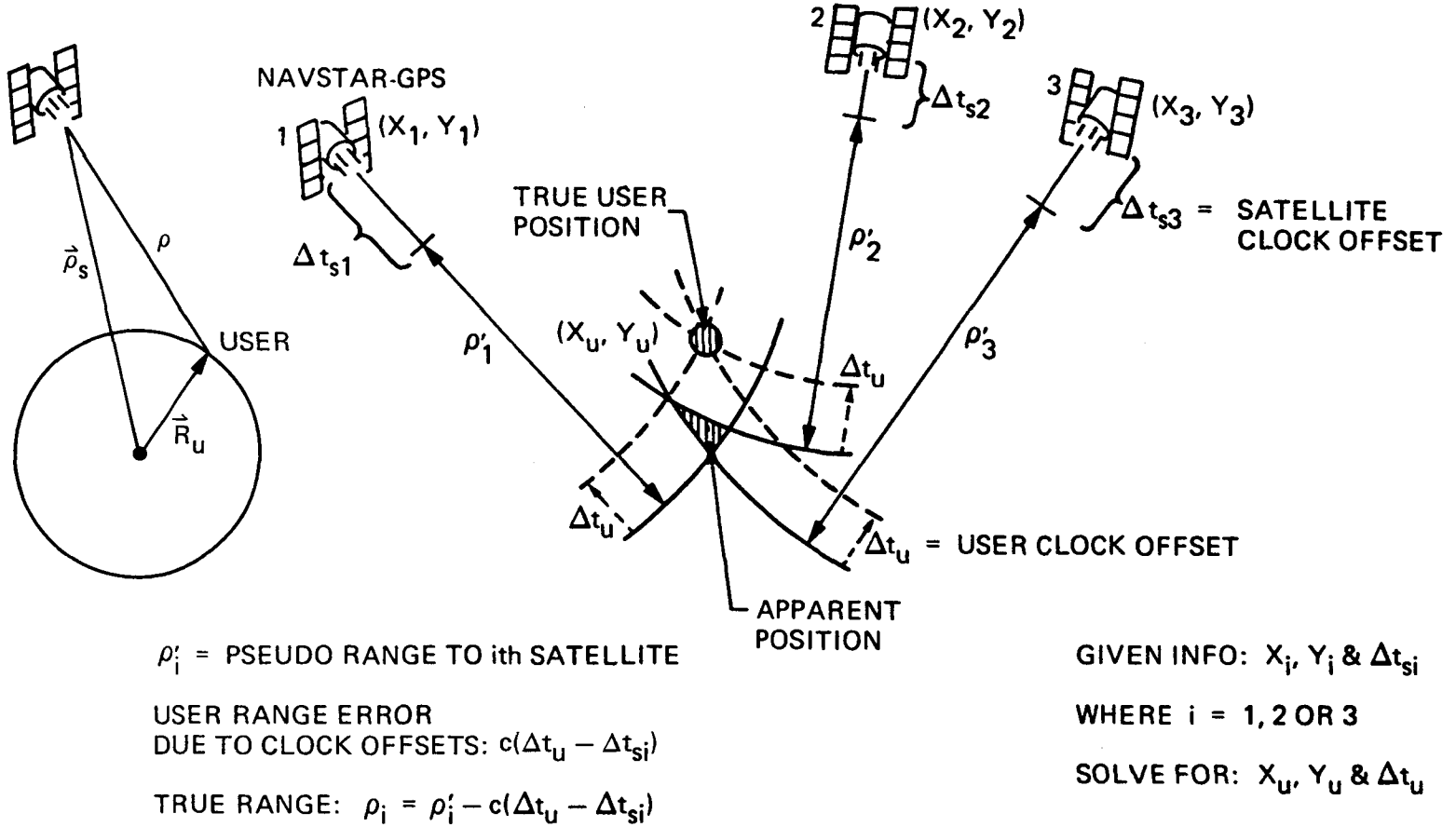

Figure 2. A two-dimensional illustration of conventional positioning using a GPS receiver having code access

signals from four NAVSTAR satellites using the coarse acquisition (C/A) code and the precision (P) code channels, the resulting measured pseudo ranges ρ'_i, permit solution of the user geocentric location, $\vec{R}_u$. Four satellite observations are necessary to solve for the three dimensional location, $\vec{R}_u$, as well as a fourth term which accounts for the user clock offset (Ref. 7).

The development of the SERIES system as described herein assumes no knowledge of the C/A or P-code modulation sequence but can deduce differential positioning information, implementing a theory very different from the design concept of conventional GPS use.

The first challenge is to extract a usable signal from the encoded L-band transmissions without a decrypting receiver. Briefly, that detection is accomplished by a delay and multiply process that recovers the chipping rates of the C/A and P-code modulations on the dual L-band carriers, as described in Section IV of this report. This type of information acquisition has a range ambiguity, unlike the pseudo-range observable derived by decrypting the GPS P-code signals. Having no dependence upon the coded form of GPS transmissions is such an advantage to a civilian user community that innovations to accommodate this ambiguous data are well worth the effort. This is particularly attractive when the resultant system can achieve a differential accuracy improvement 1000 times better than the 16m accuracy designed into the conventional GPS mode. This improved accuracy is also possible for properly designed conventional code correlating GPS receivers when used in a differential mode.

The pseudo-range ambiguities are 29.3m from P-code modulations extracted from either the L_1 or L_2 channel and 293m from the C/A code modulation which is available only on the L_1 channel. The P-code ambiguity is resolved by interpolating within the C/A code modulation to a precision of 10 meters which represents a modest 3% of the C/A code cycle wavelength and requires an amplitude Signal to Noise Ratio, SNR = 5. An ambiguity of some number of C/A cycles (wavelength, 293m) is now present which can be resolved by the use of Doppler positioning techniques accurate to 100 meters which are unambiguous. Alternately, the 293 m ambiguities can be resolved using a priori baseline information. Thus, a method has been outlined which deduces unambiguous pseudo ranges based on P-code modulation.

Consider the two dimensional case shown in Figure 2. To deduce the true user position in absolute mode, a solution of the following system of equations is performed:

$$\sqrt{(X_u - X_1)^2 + (Y_u - Y_1)^2} = \rho'_1 - c(\Delta t_u - \Delta t_{s1})$$

$$\sqrt{(X_u - X_2)^2 + (Y_u - Y_2)^2} = \rho'_2 - c(\Delta t_u - \Delta t_{s2})$$

$$\sqrt{(X_u - X_3)^2 + (Y_u - Y_3)^2} = \rho'_3 - c(\Delta t_u - \Delta t_{s3})$$

where ρ'_1, ρ'_2, and ρ'_3 indicate actual measurements of the pseudo-range from the user's receiver to the satellites which are located at the given satellite positions of X_i and Y_i and with their individual satellite clock time offsets of Δt_{si} where i = 1, 2 or 3.

For this two-dimensional case the three unknowns, X_u, Y_u and Δt_u are solved for based upon the three observations ρ'_1, ρ'_2 and ρ'_3. These measured values are subsequently combined with corrections for various time delays to produce an estimate of the true range, ρ.

The SERIES development, to be expanded upon in later sections, makes it possible to measure the pseudo-ranges ρ'_i without code knowledge. However, the satellite clock offset terms, Δt_{si}, are generally unknown for each of the satellites being observed by a user without code knowledge. To avoid the necessity of knowing satellite time, t_s, or the satellite clock offset, Δt_{si}, a pair of user stations now observes the three satellites, and the measured pseudo ranges to each satellite are differenced between stations:

$$\Delta\rho = \rho_2 - \rho_1$$

Any offset in the epoch time of satellite transmission is an error presented simultaneously to the two stations and is therefore common-mode eliminated in the differential data type (see Fig. 3). This two-station differential data type is also identical to the delay-data type developed by cross correlation signal detection in Very Long Baseline Interferometry (VLBI).

Thus, the point positioning technique producing the geocentric location of the user and the user clock offset (X_u, Y_u, Δt_u) is abandoned in favor of a technique for determining the differential location of station 2 relative to station 1. The unit vector $\hat{S}$ is located at station 1 and points to the satellite signal source at a distance ρ_1. The baseline vector $\vec{B}$ points from the antenna at station 2 to the antenna at station 1.

The satellite clock offsets are eliminated since they are common to each station, but in their place a new clock parameter appears, that of the two user clocks' offset. In general, clock 1 is not synchronized to clock 2. Because the satellites are a finite distance away from the user receivers, incoming wavefronts are spherical in shape. The VLBI geodetic experience deals with extragalactic radio sources, which are virtually at infinity and thus have planar wavefronts. As shown in Reference 8, the usual VLBI geodetic equations can be recast into a modified form by including a spherical to planar wavefront term, δ. The set of differential pseudo-range equations take on the form

$$\Delta\rho = -\hat{S}\cdot\vec{B} + \delta + c(\Delta t_{u1} - \Delta t_{u2}) + ct_{TM} \tag{1}$$

where

$$\delta = \frac{(\rho_2 - \rho_1)^2 - B^2}{2\rho_1}$$

and

$$\Delta\rho' = \rho'_2 - \rho'_1 = (c/f)(f_2T_2 - f_1T_1) + (c/f)(N_2 - N_1) \tag{2}$$

where the prime indicates a measured quantity.

The term $(\Delta t_{u1} - \Delta t_{u2})$ is the offset of clock 2 relative to clock 1 and t_{TM} is the differential time delay associated with the transmission media of

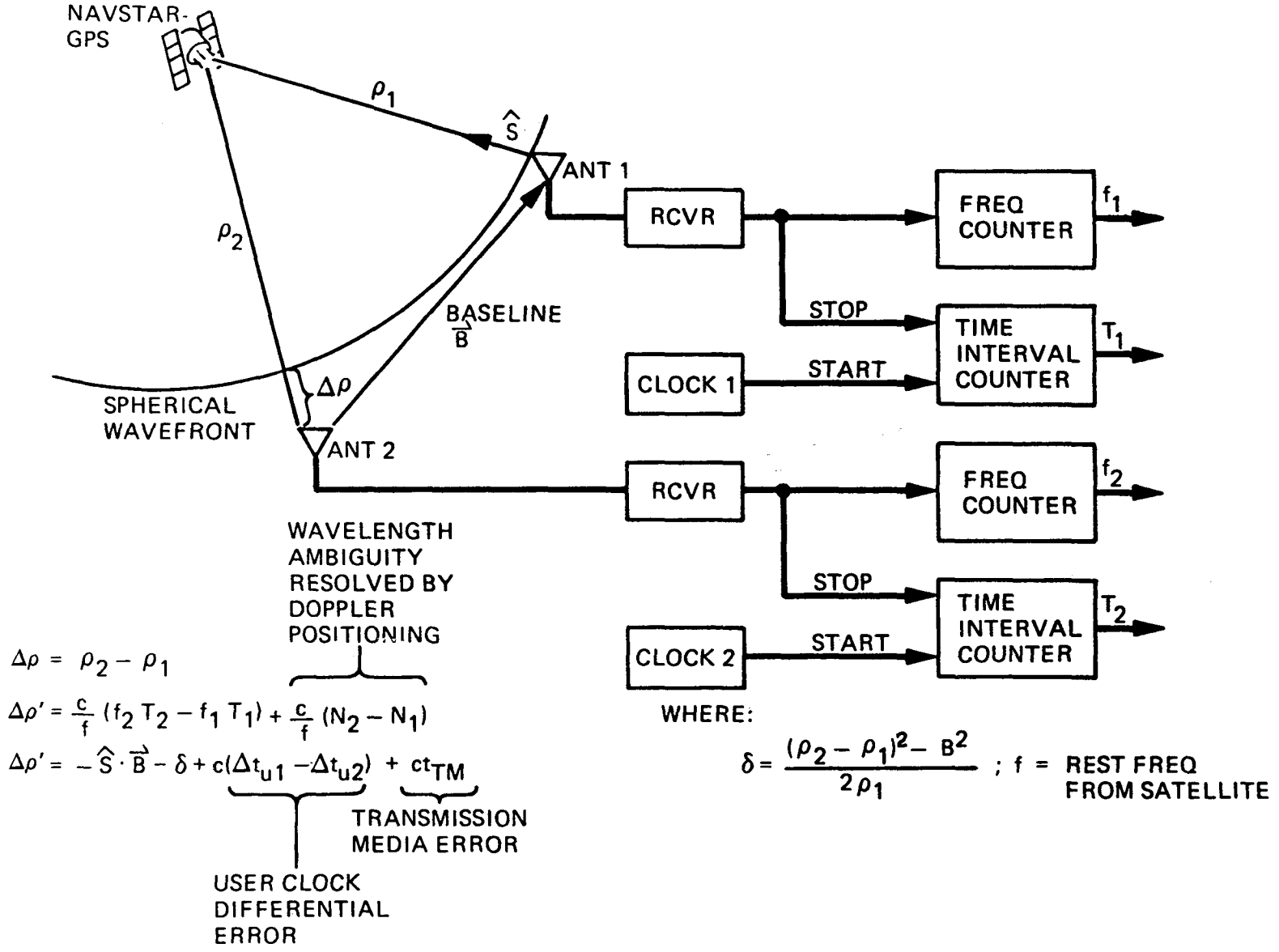

Figure 3. SERIES differential positioning geometry

the troposphere and ionosphere through which the satellite signals must pass in reaching the user receivers. The tropospheric delay calibration can be ignored, modeled, or explicitly calibrated depending upon accuracy requirements. The ionospheric delay can be explicitly measured without code knowledge by exploiting the dual frequency NAVSTAR transmissions, as will be discussed in subsequent sections. The terms N_1 and N_2 account for the phase ambiguities associated with the SERIES technique at stations 1 and 2. For example, the P-code chipping rate of f = 10.23 MHz is recovered and exhibits a phase offset indicative of the pseudo-range, ρ_i, to the satellite but with an ambiguity of the P-code wavelength. In Figure 3, the pseudo range at station 1 is formed by measuring the elapsed time from the one-pulse-per second (1 pps) event markers of clock 1 to the next occurring positive-going-zero crossing of the P-code's 10.23 MHz sinusoidal output encountered by receiver 1.

The time interval counter (TIC) indicates a value T_1 between 0 and 97.75 nanoseconds (1/10.23 MHz). The received P-code frequency will be Doppler shifted by up to 27 Hz for a stationary receiver, and the actual received frequency, f_1, is measured. The P-code fractional phase is now formed by multiplying the f_1 by T_1. The pseudo range is the wavelength (c/f) multiplied by the fractional phase,

$$\begin{aligned} \rho'_1 &= (f_1 T_1)\ c/f + N_1 c/f \\ &= \theta_1 \lambda + N_1 \lambda \end{aligned} \tag{3}$$

where N_1 c/f is the integer number of whole P-code wavelength cycles (c/f = λ = 29.3 m) between the receiver and satellite, and f is the rest frequency of the satellite P-code clock.

In this process it has been assumed that the geocentric location of receiver 1 ($\vec{R}$) the unit vectors from receiver 1 to the satellite, ($\hat{S}$), and the range from receiver 1 to the satellite ($\vec{\rho}_i$) are known quantities.

Receiver 2 outputs are now measured relative to clock 2 and the pseudo range from station 2 becomes

$$\rho'_2 = (f_2 T_2)c/f + N_2 c/f \tag{4}$$

The differential pseudo range is now formed as

$$\Delta\rho' = \rho'_2 - \rho'_1 = (f_2 T_2 - f_1 T_1)c/f + (N_2 - N_1)c/f \tag{5}$$

The true differential pseudo range, $\Delta\rho$, is functionally dependent upon the baseline as indicated in equation (1).

The problem is now the determination of the ambiguity of whole cycles, N c/f. Figure 4 illustrates in two dimensions the physical situation of three NAVSTAR satellites following each other around the Earth in their 12-hour period circular orbits. The observer is located at $\vec{R}$ and the satellites are located at $\vec{\rho}_{s1}$, $\vec{\rho}_{s2}$ and $\vec{\rho}_{s3}$. The NAVSTAR satellites each transmit the same frequency (f_T), and the observer is assumed to have a receiver with an oscillator synchronized to the same UTC frequency scale. The measured Doppler frequency is

$$f_M = f_T\left(\frac{V_s}{c}\right) \cos(\alpha) \tag{6}$$

The velocity vector projections along the line of sight cause the Doppler shift effect. Consider a simplification of a non-rotating Earth or a possible observer at a very high latitude so that the Earth's rotational velocity is very small compared to the satellite's velocity along its orbital path. Each value of the Doppler frequency, f_M, measured at time t, allows the look-up or computation from ephemeris elements of the satellite state vector, containing the position $\vec{\rho}_{si}$ and velocity $\vec{V}_{si}$. Therefore, all possible places where the observer could be located are on the surface of a cone whose vertex is at the satellite position $\vec{\rho}_s$, and whose axis of rotation lies along the satellite's velocity vector. The half apex angle of the cone is given by

$$\alpha = \cos^{-1}\left[c\, f_M/(v_s f_T)\right] \tag{7}$$

Since Figure 4 illustrates a two-dimensional situation, the intersection of the cones with the plane of the figure reduces the loci of possible positions

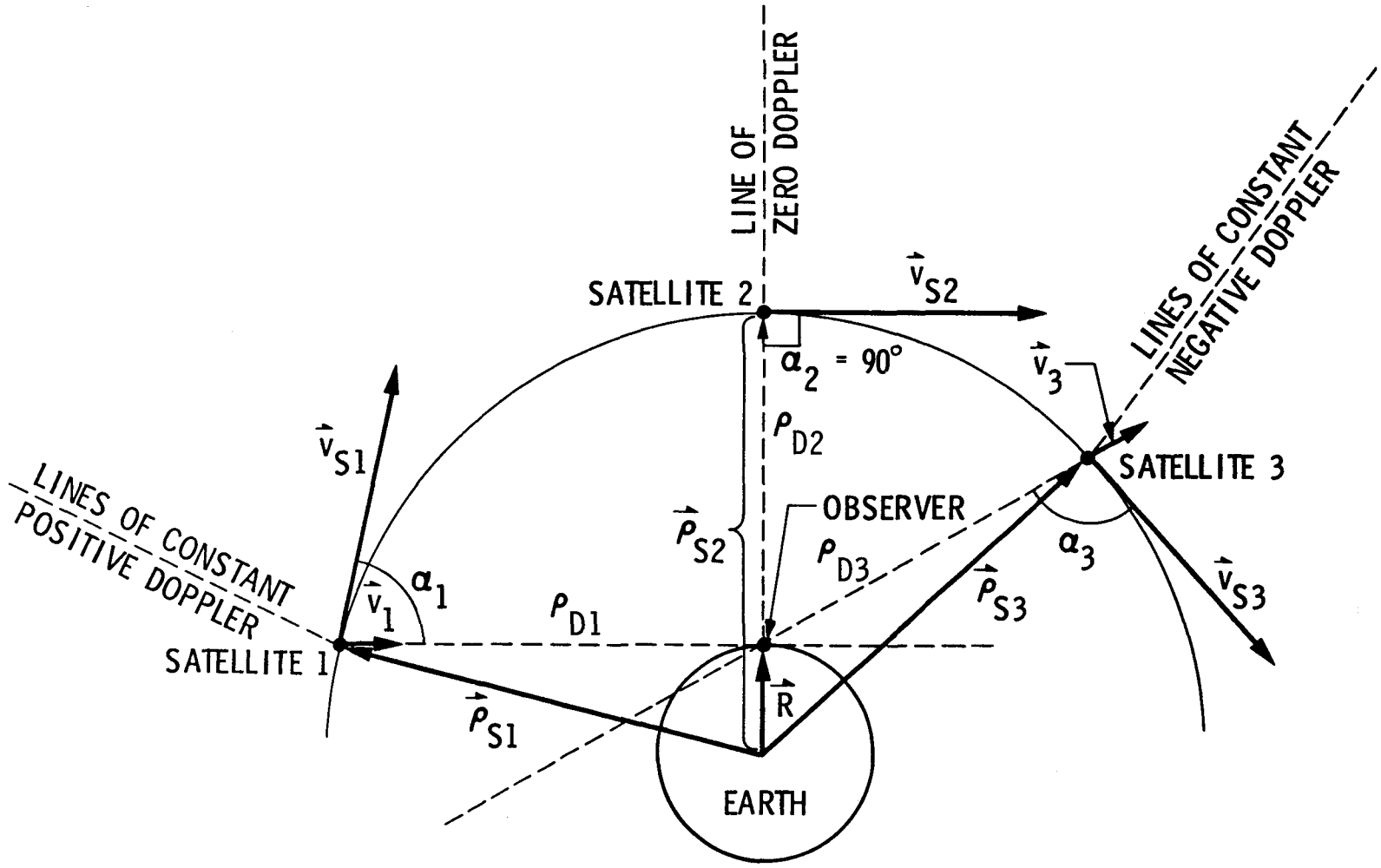

Figure 4. SERIES Doppler positioning geometry

to lines of constant Doppler. The intersection of the lines of possible position from satellites 1 and 3 are sufficient to determine the observer position $\vec{R}$. Satellite 2 is shown at the special case of zero Doppler occurring at the time of closest approach (TCA) so that the observer must lie in a plane defined by the normal to the satellite 2 velocity vector. Actually, two satellites would have been sufficient to determine $\vec{R}$ given the assumption of synchronized receiver and satellite oscillators, but the third satellite adds redundancy or an additional observation to solve for the receiver reference oscillator frequency offset relative to the assumed synchronized satellite transmitted frequencies f_T.

Having determined $\vec{R}$ and having $\vec{\rho}_s$ as a given, the Doppler pseudo range $\rho'_D = \left| \vec{\rho}_s - \vec{R} \right|$ is deduced and equated to Equations (3) and (4). Thus,

$$N\ c/f = \rho_D - c/f(f_M T) = \left| \vec{\rho}_s - \vec{R} \right| - (f_m T)c/f \qquad (8)$$

is a solution for determining the ambiguity of the whole cycles, N c/f.

IV. IMPLEMENTATION

The innovations to be described were developed primarily in pursuit of extraterrestrial geodesy by a system called Satellite Emission Range Inferred Earth Surveying (SERIES) (Reference 8). However, the term SERIES used in these descriptions will be considered as a generic term. Imagine one or more SERIES devices receiving signals from four or more GPS satellites. Each station is equipped with an antenna, a receiver and a data system (see Figure 5). The challenge is to extract information from an encrypted spread spectrum, which is bi-phase modulated with full carrier suppression using an unknown pseudo random noise (PRN) code sequence. It is known (Reference 6) that the carriers and rate of digital modulation transitions are controlled by the satellite-borne atomic frequency reference. All GPS satellites have an identical rate of 10.23 mega-transitions per second which is termed the chip rate of the P-code channel. Two other modulations are also present: 1.023 MHz, called the coarse acquisition channel (C/A), and a 50-bit-per-second telemetry channel containing satellite ephemeris data. Dual frequency bands are provided for ionospheric calibration, and are L_1, centered at 1575.42 MHz, and L_2, at 1227.6 MHz. These are generated by multiplying the 10.23 MHz signal by 154 and 120, respectively.

To exploit these signals without code sequence knowledge, a nonlinear detection scheme is used. The P and C/A code modulation transitions are recovered when a delay and multiply method is employed (Figure 6). The effect is to collapse a broadband 20.46 MHz signal (10.23 MHz, double sideband) into a simple sinewave. Such methods have been common practice (References 9 and 10) to demodulate telemetry data synchronously, where the recovery of the telemetry bit clock frequency is merely a means to the end of recovering the telemetry bit stream. In the SERIES implementation, the actual P-code and C/A code bit sequences are not explicitly used. The strategy is to exploit the chip rate as a type of coherent range code which has ambiguities that can be resolved. Specifically, by exploiting the fact that Doppler Positioning is virtually unique, the ambiguities in the phase measurement of the C/A code can be resolved, which in turn enables the resolution of P-code cycle ambiguities.

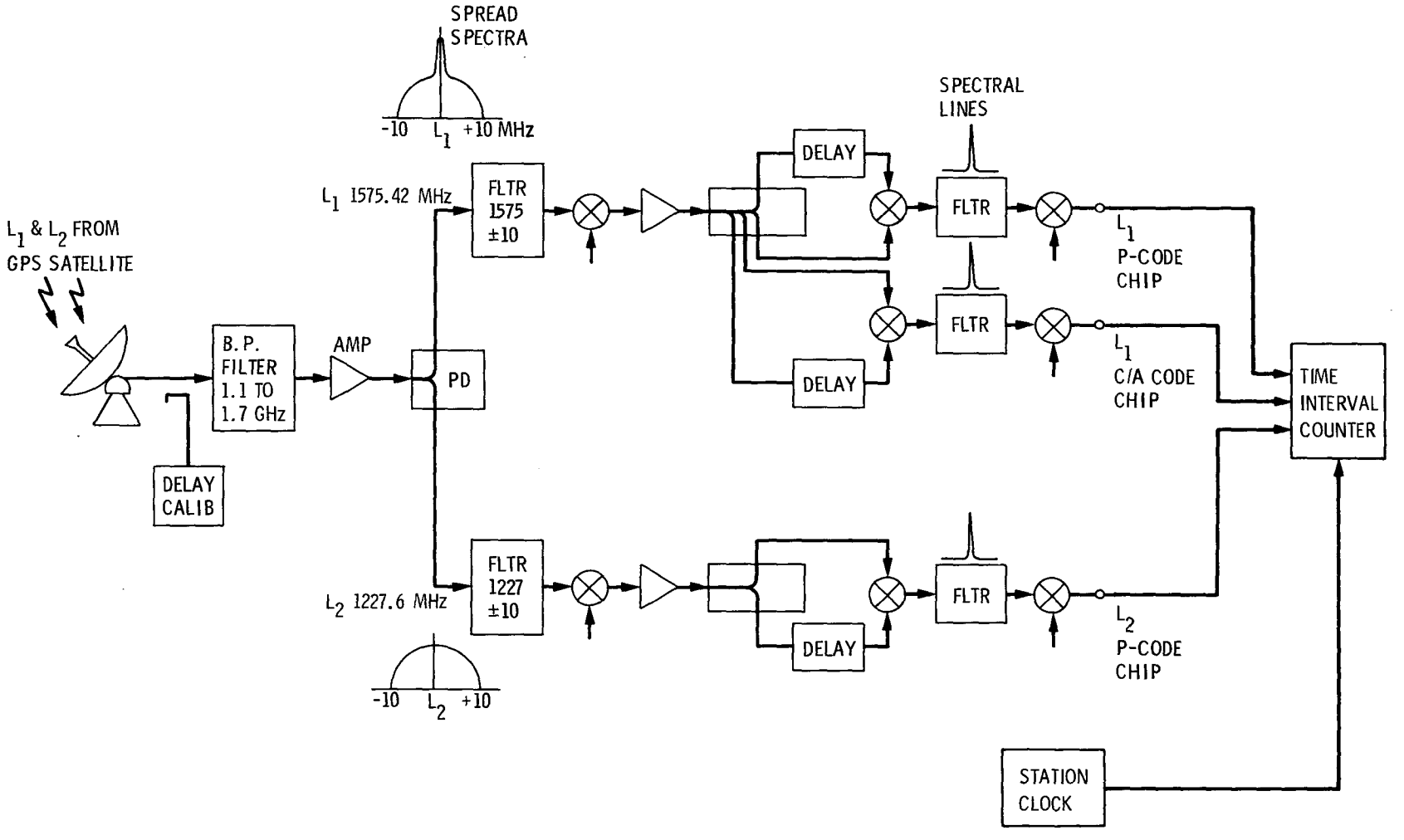

Figure 5. SERIES simplified block diagram

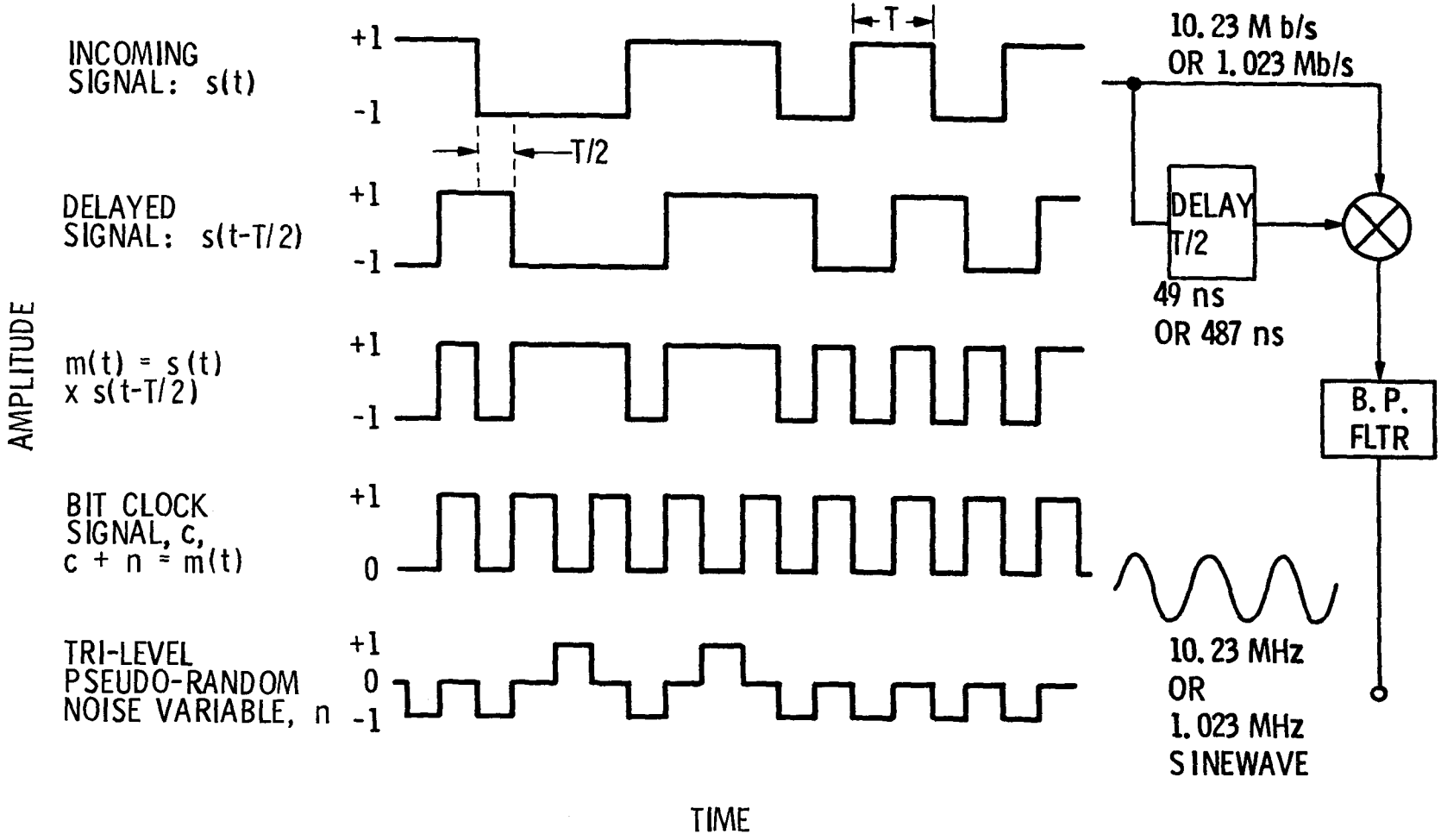

Figure 6. SERIES delay and multiply technique

For some applications, there is a desire to have access to the L-band RF carriers and the P and C/A-code channels' sub-carriers, all of which have been coherently derived from the on-board spacecraft atomic frequency references. Because of the needs of the conventional GPS mission, these signals are stable to better than 10^{-12} sec. at 100 seconds averaging time (Reference 11).

Using these signal-squaring techniques, with a half-chip time delay in the case of the sub-carriers, it is possible to recover the P-code modulation rate of 10.23 MHz at both the L_1 and L_2 channels. These P-codes exhibit Doppler shifts that span from 0 to ±27 Hz. The C/A-code modulation of 1.023 MHz, usually present only on the L_1 channel, is similarly recovered and has a Doppler shift of 0 to ±2.7 Hz.

A major feature of the SERIES technique is now evident, that of information compression. In the beginning, there was a spread spectrum of 20.46 MHz width of unknown modulation, and now all the information necessary for pseudo ranging and ionospheric calibration is contained in sinewaves which are confined to a relatively narrow bandwidth. Specifically, for an Earth-fixed observer all the P-code information is contained within a 54 Hz bandwidth, and the C/A channel within 5.4 Hz.

Imagine now a receiver that has input to it a signal from a single GPS satellite. The C/A channel output of the 1.023 MB/S chipping rate is connected to the stop channel of a time interval counter (TIC) (Figure 5). This counter is started by a 1 pps signal from the receiver clock. The range of the satellite to the receiving antenna is now indicated by the time interval counter, modulo 978 nanoseconds (the period of 1.023 MHz) with an unknown possible bias between the satellite and the SERIES receiver clocks. A second receiver can now perform the same measurement relative to its own clock (Figure 7). By calculating the following

$$(T_2 f_2 - T_1 F_1)$$

a differential phase delay observation is created where T_i is the time interval counter value of the i^{th} station, and the product $T_i f_i$ is the fractional phase measured at that station. This is identical to the delay

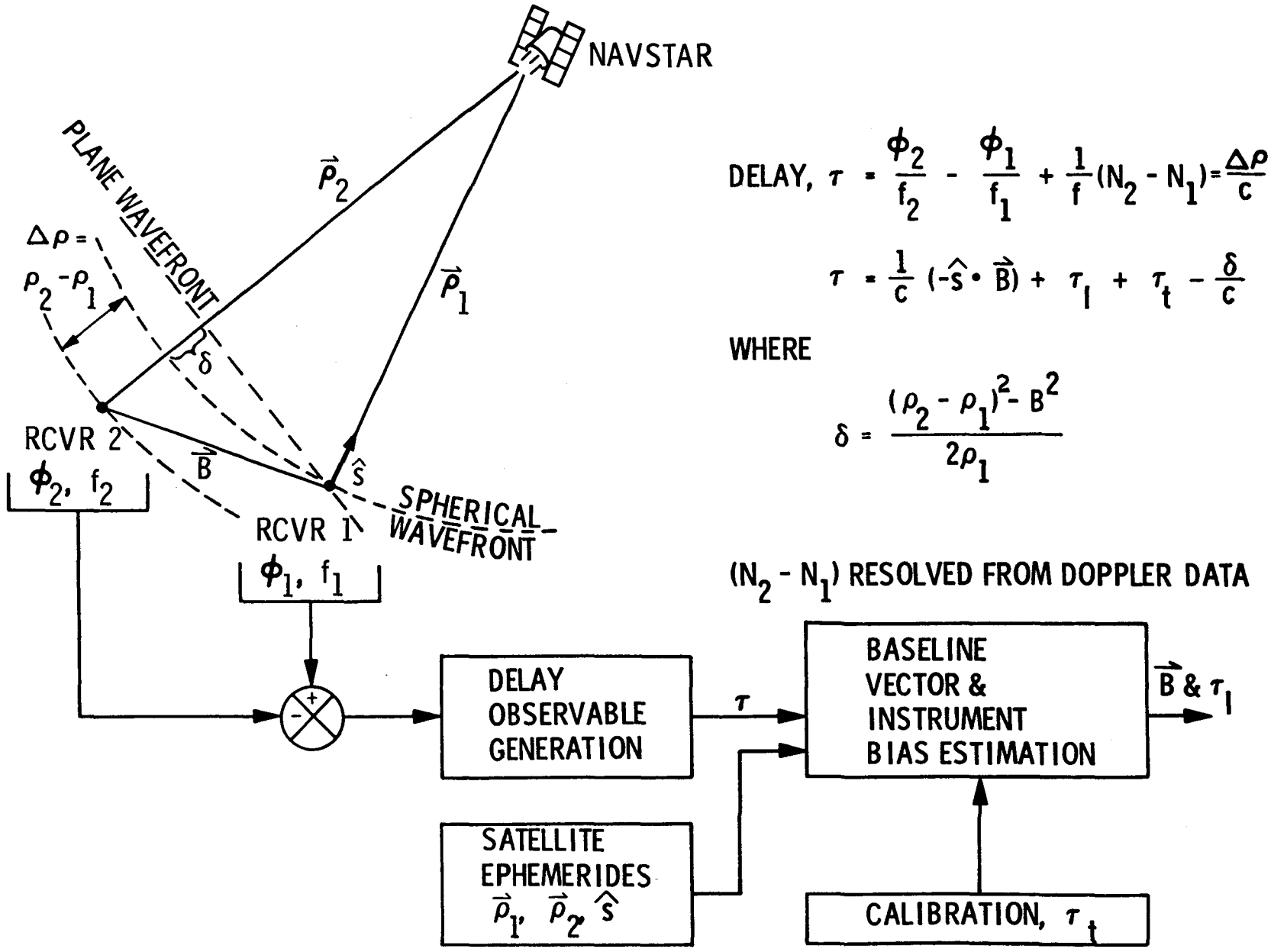

Figure 7. A schematic representation of the SERIES baseline solution

data type of VLBI (Reference 12) for which considerable baseline measurement experience exists (Reference 13). Note that the possible C/A-code phase bias in the satellite now vanishes, but in its place another bias appears which is the difference of clock epochs between station 1 and 2. The delay observable created by differenced C/A-code ranging is ambiguous at the C/A-code wavelength of 293 meters. Similarly, this same procedure could be employed using the P-code which would introduce ambiguities in the delay of 29.3m. For convenience and reduced cost of implementation, the recovered sinewaves are coherently down-converted to lower frequencies where the performance of simple time interval measurement equipment is quite adequate (Figure 5).

The next step is to estimate the baseline vector and deduce the time offset of the station 1 clock relative to the station 2 clock. The conceptual approach is identical to that employed in quasar VLBI geodesy (Reference 13). Consider four or more GPS satellites above the horizon common to stations 1 and 2. Four delay observations are developed by differencing digital time interval counter readings scaled by the Doppler frequency. All of the GPS satellites are widely separated in the sky, and thus the geometry and the four delays allow for a simultaneous estimation of the three-dimensional baseline vector and the relative clock bias between the stations (X, Y, Z, Δt). The strategy here is to make four delay observations as rapidly as possible so as to minimize the effect of receiver clock instabilities. The clock error contribution grows linearly with the total time required to observe the four or more GPS satellites.

V. DIFFERENTIAL OBSERVATIONS

An important data type is differential Doppler and differential pseudo ranging extracted either from the received carriers or from the P or C/A channels. Differencing automatically removes any possible phase or phase rate biases which might originate in the GPS satellites, because a bias which may be unique to one satellite is simultaneously recorded by each user station and is subsequently cancelled in the difference. Operating in a differential mode also reduces the sensitivity of the baseline vector determination to the uncertainties within the satellite ephemeris. Orbital errors contribute to the baseline error and are attenuated by the ratio of the baseline length to satellite height, nominally 20,000 km (Reference 14). Thus, for a 100 km baseline separation between receivers, a 10 meter satellite orbit uncertainty at its 20,000 km orbital position can contribute, with worst case geometry, 5 cm uncertainty to the baseline determination.

VI. IONOSPHERIC CALIBRATION: DUAL P-CODE CHANNELS

The L-band region of the electromagnetic spectrum contains substantial ionospheric delay effects when considering the sub-decimeter baseline accuracy requirements of geodesy. In an uncalibrated mode, the L_1 channel at 1575 MHz would experience approximately 15m of zenith range delay or up to 40m of delay at low elevation angles during active ionospheric conditions (zenith columnar contents of 10^{18} electrons per m^2). In an uncalibrated Doppler positioning mode, using the SERIES method, the L_1 channel would be disturbed by approximately 10 meters of positioning-equivalent error which results from a columnar electron content rate of change of $6x10^{17} el/m^2$ per hour.

Clearly, the dual channel availability of NAVSTAR must be used to explicitly measure the ionospheric delay and delay rate effects along the line of sight to the satellite being observed. The differential, $L_1 - L_2$ frequencies, while not being optimum for measuring the ionospheric delay, have sufficient separation for determining the dispersion effect with the required precision.

In an earlier form of experimentation (Reference 15) the SERIES ionospheric calibration used an analog cross-correlation approach which exploited the fact that the identical P-code modulation sequence is coherently transmitted by the NAVSTAR satellites on both the L_1 and L_2 GPS channels (Reference 6).

The ionospheric columnar content was measured by intentionally delaying the first arriving L_1 signals and then cross-correlating with the L_2 channel. The delay in the L_1 is made adjustable to compensate for the differential delay experienced in the L_2 channel. When the output of the correlator is a maximum, the variable delay value is the ionospheric delay. While the technique was functional, it suffered from two difficulties: The measurement was difficult to calibrate to 0.1 nanoseconds and it was vulnerable to changes in the NAVSTAR transmission format. For example, the GPS satellites could conceivably be reconfigured so as to broadcast different portions of the P-code sequence on L_1 and L_2 thus destroying the possibility of obtaining an output by inter-channel cross correlation.

A more reliable approach was to exploit the 10.23 MHz P-code bit transition rates separately derived from the L_1 and L_2 channels. The 10.23 megabit-per-second (MB/S) code chip rate is directly derived from the on-board atomic frequency references and used to coherently modulate L_1 and L_2. Although the actual code sequence or code phasing might be altered, it is likely that the P-code chip rates of L_1 and L_2 will not be changed. Thus, the phase of the code transitions are probably in coincidence or with simple constant offsets in the satellites and will therefore experience ionospheric dispersion in the same manner that the code sequence is differentially delayed in the previously mentioned inter-channel correlation approach.

A digital time interval counter and/or a phase measuring device is used to determine the lag of the L_2 channel relative to the L_1 channel to determine the columnar content of the ionosphere. This SERIES subsystem has been given the name SLIC for Satellite L-band Ionospheric Calibration (Figure 8), and is a potentially powerful tool for mapping ionospheric conditions.

Consider the P-code transitions at L_1 and L_2 to be phase coincident at the satellite's location. The L_1 and L_2 channels then experience the ionospheric dispersion because of their 347.82 MHz of frequency separation. The physics of this situation are discussed in Reference 16 and summarized as follows: The group delay effect is in general, $t_g = AI/cf^2$, where

A = 40.3 in MKS units
I = columnar electron content, electrons per m^2
f = radio frequency, Hertz
c = speed of light, meters per second
t_g = ionospheric time delay, seconds

The SLIC observable is the differential group delay (T_g) between L_1 and L_2:

$$T_g = t_{g2} - t_{g1} = AI/c \left[(1/f_2)^2 - (1/f_1)^2\right]$$

Consider now the extreme conditions of the ionosphere. The minimum zenith content to be expected is $I = 0.5 \times 10^{17}$ electrons/$meter^2$ which will

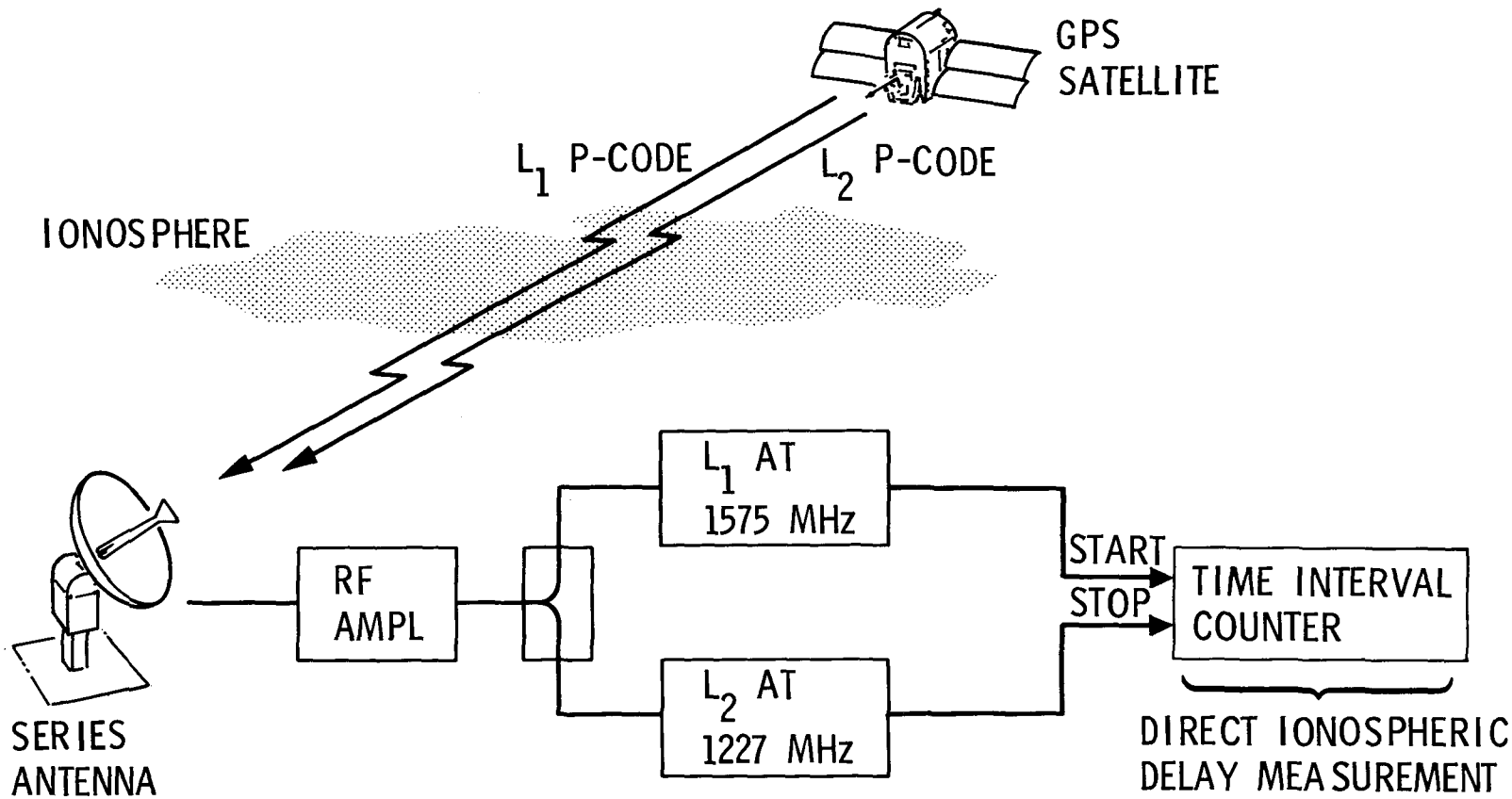

Figure 8. SERIES technique for measurement of the columnar charged particle content

result in T_g(min) = 1.75 nanoseconds. At a maximum, the zenith content could approach 10^{18} el/m^2 and observing at a low elevation angle causes a columnar content of 2.5×10^{18} el/m^2, and results in T_g(max) = 87.5 nanoseconds. Exploiting the P-code in this manner has an ambiguity of 97.75 ns, and thus care must be exercised to avoid ambiguous measurements in high ionospheric content situations.

In geodetic missions, calibration must be applied to the pseudo-range observable at either L_1 or L_2. The ionospheric delay on L_1 is $t_{g1} = 1.54\ T_g$. Thus, 10^{17} el/m^2 results in T_g = 3.5 ns or 105 cm path equivalent difference between L_1 and L_2 (267 cm path delay on the L_2 channel minus 162 cm path delay on the L_1 channel).

The SLIC error sources contain three major elements: (1) receiver noise, (2) receiver delay, and (3) possible biases in the NAVSTAR at the time of transmission. The measures taken to compensate for these error sources are as follows:

(1) Using a 1.5 m diameter antenna provides more than adequate signal strength, and the differential phase shift between the L_1 and L_2 channels is measured to within 0.1 ns RMS or better with one second of averaging using the Bipolar transistor preamplifier, corresponding to a columnar content of 3×10^{15} el/m^2 or 4.6 cm of pseudo range calibration on the L_1 channel. Thus, to achieve a two centimeter precision in pseudo ranging calibration, 5 seconds of SLIC data must be averaged.

(2) To measure the differential phase behavior of the SLIC receiver itself, a GPS satellite simulator consisting of a PRN (pseudo-random noise) sequence is modulated onto carriers at L_1 and L_2 and injected into the first RF amplifier, and the data system processes the signal in a manner identical to the reception of the NAVSTAR signals. In this way the dissimilarities between L_1 and L_2 signal paths are measured with a precision of 0.06 ns to achieve a 2 cm accurcy in the SLIC receiver delay.

(3) According to the specification of the Block I NAVSTAR satellite (Reference 17), the relative phasing of the P-code transmissions on L_1 and L_2 channels will vary by less than 1.5 nanoseconds. Such a time difference in transmission will cause a bias in the deduced total columnar content equivalent to 3×10^{16} el/m^2 but will have no effect upon the SERIES determined baseline vectors performed in a two-station differenced pseudo range mode since any satellite biases are common-mode rejected.

Important features of the SLIC method are listed below:

1) Total columnar electron content measurement with a precision of 10^{15} el/m^2 with 10 seconds of averaging and an accuracy dependent upon phasing in the NAVSTAR, limited to approximately 3×10^{16} el/m^2.

2) No P-code digital sequence knowledge required.

3) No dependence upon orbit kinematics of the NAVSTAR.

4) No modeling of geomagnetic fields or unsensed electrons as with the Faraday Rotation method.

5) No active elements as with ionosondes or topside sounders aboard Earth-orbiting spacecraft.

6) Modest instrumentation requirements, with options for omni-directional reception.

7) Columnar content measurement from a single station; no cross-correlation between two stations to achieve signal detection as in the VLBI method.

8) A single satellite pass allows horizon-to-horizon sampling of the ionosphere in 6 hours; the full 18 satellite constellation will allow a continuous sampling in at least four directions (perhaps as many as seven) from every location on the Earth's surface.

VII. BASELINE ESTIMATION SOFTWARE

Baseline estimation software has been written to allow the evaluation of the SERIES receiver engineering tests. This program allows the determination of a baseline between two SERIES stations, the clock offset between the stations, and the approximate location, in the WGS-72 frame, of each station.

Data input from the SERIES stations to the baseline estimation software consists of time tagged pseudo ranges to the GPS satellites as well as measurements of the ionospheric delays along the lines of sight to the GPS satellites. Other ancillary data can be entered such as surface measurements of barometric pressure, temperature, relative humidity, or water vapor radiometer measurements of water vapor delays.

The baseline program also requires ephemeris information. The orbits determined post facto by the Naval Surface Weapons Center (NSWC) are currently being used for SERIES baseline tests. These orbits, with approximately 10-m errors, are adequate for precision determinations of baselines up to 100 km.

The baseline program operates on singly differenced ranges, i.e., the difference in simultaneous pseudo ranges between two stations to a GPS satellite. These differences are formed and compared with the modeled differences based on the ephemerides, the a priori station locations and clock offsets. The three components of the baseline vector and the clock offsets are adjusted so that the least squares residuals are obtained.

The data can be sent over phone lines so that a near-real time (within 1 hour) baseline solution can be obtained. Presently, this near-real time solution does not have the precision ephemeris information available, leading to degraded baseline accuracy. The a priori ephemeris is available at the time a baseline is measured, while the post-fit ephemeris is generally available two weeks hence.

VIII. SERIES TEST SEQUENCE

The testing program was designed to allow a sequential check of suspected system error sources (see the listing below).

Experiment	System Component Tested
Single Station	Instrumentation
0 Baseline	Instrumentation + Baseline Estimator
150 M Baseline	Instrumentation + Clock + SNR + Multipath
150 M Common Clock	Isolates Clock Error Source
150 M Attenuated	Isolates SNR Error Source Signal
150 M Long Track	Sensitive to Multipath
21 KM (DSS13/14)	Test Field Operation of Mobile Units
21 KM (Clock Sync)	SERIES Clock Sync Demonstrated
Faraday Co-Location	SERIES Ionospheric Calibration Validated
171 KM (JPL/Goldstone)	Tests Dependence of Errors on Baseline Length, Atmospheric Delay Models, Ephemeris Errors

A. SINGLE STATION TESTS

Single station tests were performed to indicate whether receiver stability was adequate to obtain baseline measurement results with few cm precision. The SNR (Signal to Noise Ratio) of the GPS satellite signals in the receiver Intermediate Frequency (IF) band were also measured in single station tests. This was compared with the output SNR of the reconstructed code clocks in order to verify that the SERIES code clock recovery technique was operating at or near the theoretically predicted performance level.

Single station tests were repeated throughout the test sequence in order to periodically validate instrument performance.

B. 0 BASELINE

The 0 baseline tests were performed with the output signal from a single antenna being split to provide inputs to the two SERIES receivers. One

Rubidium frequency standard was used to provide the reference clock for both of the SERIES receivers. The RMS scatter in the baseline lengths was 1 cm, which is less than the 3 cm predicted by the SNR if independent noise is present in each receiver. This is due to the fact that much of the noise in the 0 baseline experiment is correlated between the two receivers and, therefore, cancels. The mean measured baseline length of 5 cm is thought to have been caused by electronic cross-talk between the two closely situated receivers.

C. 150 METER BASELINE

As can be seen in Figure 9, a greater separation to a 150m baseline increased the RMS scatter to 3cm, which is the value expected from the SNR error combined with the clock jitter error resulting from the Rubidium vapor frequency standards. The mean of the SERIES length measurements differed from a conventional survey by 0.3cm.

The experiments conducted with a common frequency standard for the two stations showed no significant improvement over those which used separate clocks. This is consistent with the expected 1-cm baseline error contribution due to clock noise.

A baseline measurement was conducted with a known attenuation added to the satellite signal input to the first amplifier. This caused a known degradation of the system SNR. From this information, the increase of that part of the RMS scatter of delay residuals in the baseline fit due to system SNR could be predicted. By noting the actual increase in the RMS of the delay residuals, it was determined that, in fact, the system noise from the first amplifier was the dominant error source in the SERIES GPS receivers.

The errors due to the presence of multipath signals are expected to be small for a GPS receiver with a highly directive antenna. These errors are difficult to estimate, and so were measured by having both stations track a common satellite while subjecting one station to likely multipath sources. In this experiment media delays, geometric effects, etc., were largely common-mode rejected. The multipath effect was determined to cause less than a 1-cm baseline error, using the SERIES 1.5-m antenna.

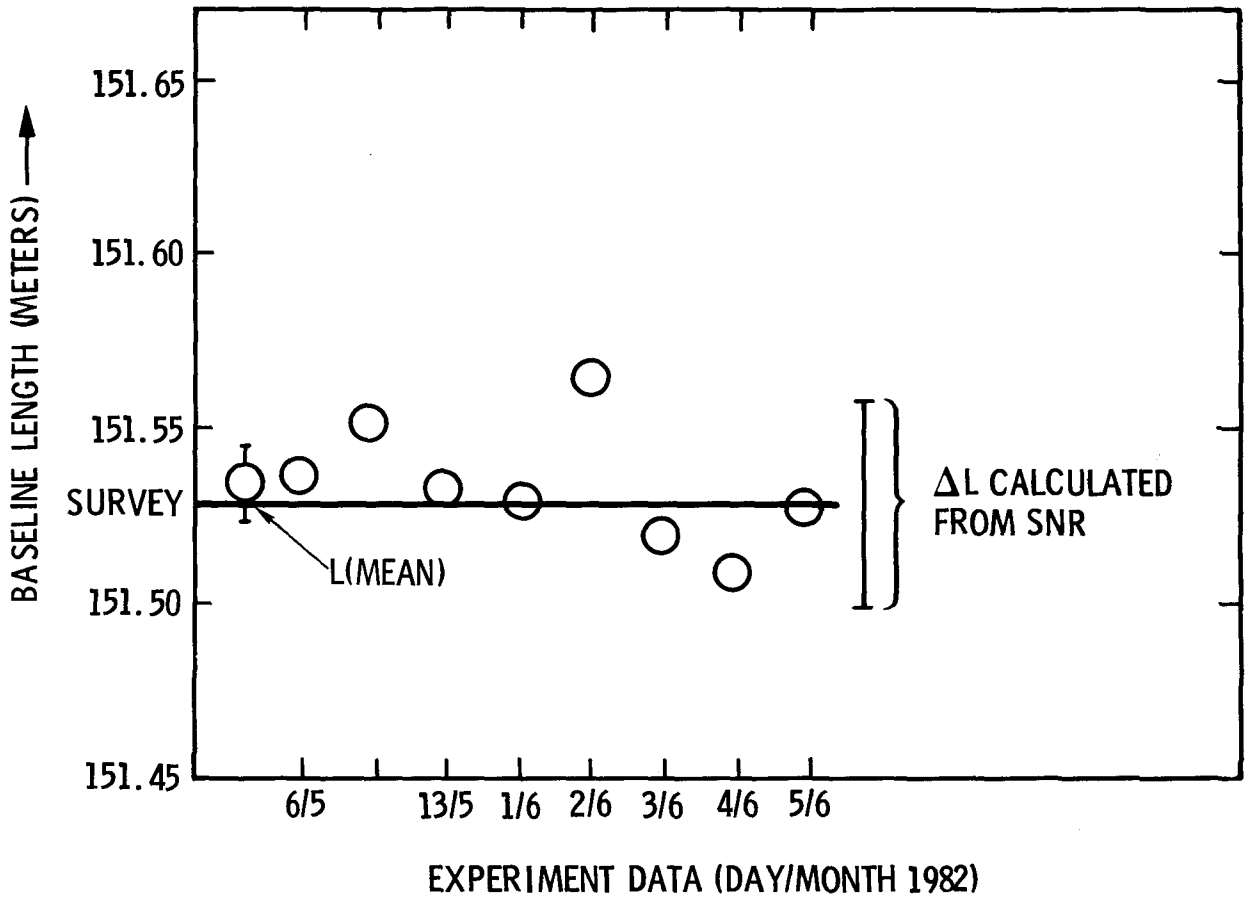

Figure 9. SERIES 150 m baseline length measurements. Each circle without error bars represents a solution using 1.25 to 1.75 hours of data taken on a constellation of five GPS satellites, mutually visible over Southern California. The scatter among these solutions is consistent with the SNR error bar. The mean length agreed with the conventional survey to within the SERIES errors, with a difference of 0.3 cm.

D. 21 KM BASELINE

For the proof-of-concept system, the SNR errors still dominate at the 21km baseline, with 4cm RMS scatter of the solutions for baseline length. The comparison between the composite survey (combined VLBI and conventional measurements) and the SERIES measurement, in Earth fixed coordinates, is shown in Figure 10. The errors in the composite survey are estimated to be less than 5 cm in each component. The errors in the components of the SERIES determination vary. The north-south component of the SERIES baseline is quite well determined, while the east-west and vertical components are less well determined. This can be explained by simple geometric factors. The set of five operating GPS satellites available during the tests described here formed a constellation over California which is nearly aligned along the north-south direction. This geometry provides for a weak solution in the east-west component of the baseline. A similar argument can be made for the local vertical component, as obviously no satellites can be observed in the local "down" direction. This effect is, of course, also present for the other baselines which were measured. The existence of the eventual full 18 satellite GPS system in the late 1980`s will offer improved geometric as well as time coverage.

E. 21 KM - CLOCK SYNCHRONIZATION

While the SERIES stations were on the 21 km baseline, two experiments were performed to demonstrate the measurement of the clock offset between the two station clocks (Ref. 5). The usual SERIES multi-parameter solution contains a determination of clock offset and rate as well as the baseline vector separating the two stations. This solved-for clock offset contains contributions from the differential receiver delays at the two SERIES stations. In addition, the solved-for delay includes contributions from the phases of locally generated heterodyne signals. Ancillary measurements were taken during the clock sync experiments to calibrate the effect of each SERIES station`s heterodyne signal phase. In order to measure the differential instrumental delays between the two receiving stations, they were brought together for a calibration run on a 2m baseline. The error in the SERIES measurement of clock sync was estimated to be 1 ns (10^{-9}sec). This is

COORDINATE	*COMPOSITE SURVEY	SERIES (ERROR)	SERIES - COMPOSITE
LENGTH (METERS)	21463.655	21463.667 (±0.018)	+0.012
X (METERS)	-2531.786	-2531.829 (±0.021)	-0.043
Y (METERS)	14090.312	14090.266 (±0.027)	-0.046
Z (METERS)	15991.925	15991.960 (±0.021)	+0.035

* SURVEY IS COMPOSITE OF VLBI + CONVENTIONAL SURVEY MEASUREMENTS

Figure 10. Comparison of SERIES and composite measurements of the 21 km baseline

dominated by errors in measuring the differential instrumental delays between the two receivers. On longer baselines, the ephemeris errors would also become important. They would be expected to contribute a 5 ns error to the clock sync measurements on a 3,000 km baseline if 10-meter orbit errors are assumed.

During the two SERIES clock sync experiments, a Rubidium vapor frequency standard was used as a traveling clock to allow an independent check on the SERIES clock sync results. To obtain accurate results with the traveling clock, three round trips were made between the two SERIES stations. At each visit of the traveling clock to a SERIES station, the epoch of the traveling clock was compared to the SERIES station clock using a time interval counter to measure the offset of the clocks. Care was taken to insure that trigger levels were set to the same levels on each visit and the same coaxial cables were used at each station. The offset between each station clock and the traveling clock was later fit to a second order polynomial so that the time offset between the two station clocks could be determined at a common epoch. The traveling measurement clock error was estimated to be 0.7 ns.

When the clock offsets obtained with the SERIES technique were compared with the independent traveling clock measurements, interpolated to the same epoch, agreement was within one nanosecond for each of the two clock sync experiments (Fig. 11). (This agreement was obtained after adjusting the 977-ns ambiguity of the C/A code chip period present in the SERIES receiver.)

F. FARADAY CO-LOCATION - SLIC TEST

A schematic representation of the operating principle for the SERIES L-band Ionospheric Calibration (SLIC) technique is shown in Fig. 12. In order to demonstrate this technique for measuring the columnar free electron content in the ionosphere, data were taken with the SERIES station co-located with another system capable of measuring the ionospheric content (Faraday Rotation). Figure 13 shows a comparison of the two techniques for one day of data. Note that each technique measures the total electron content along different lines of sight, and these are then mapped to the zenith content. The agreement between the two techniques is about 10^{16} e/m^2 when the two lines of sight are close and, therefore, mapping errors are small.

	$t_{STA\ A} - t_{STA\ B}$ SERIES RECEIVER	$t_{STA\ A} - t_{STA\ B}$ TRAVELING CLOCK	DIFFERENCE BETWEEN 2 TECHNIQUES
23 AUG 82 14:36:45 PDT	-189.7 ns	-190.3 ns	+0.6 ns
24 AUG 82 14:00:45 PDT	-1302.0 ns	-1301.4 ns	-0.6 ns

Figure 11. One nanosecond (10^{-9} second) agreement was observed on each of two experiments in which a traveling clock was used to verify SERIES clock synchronization measurements made on the 21 km baseline.

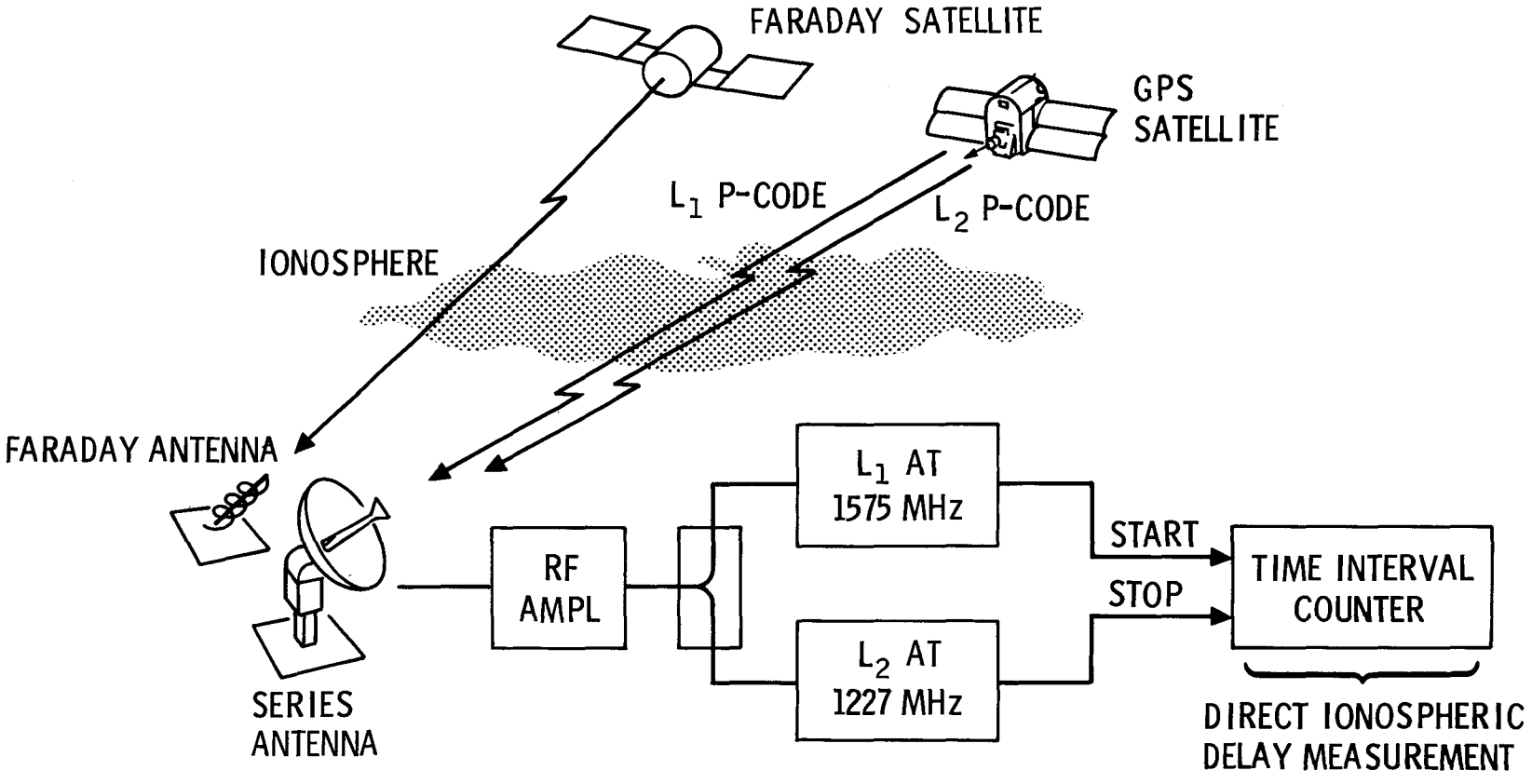

Figure 12. The P-codes are nearly in phase when transmitted from the GPS satellites, but suffer a differential delay due to the presence of free electrons in the ionosphere. By measuring the magnitude of this differential delay, the SERIES station is able to determine the columnar content of free electrons in the ionosphere.

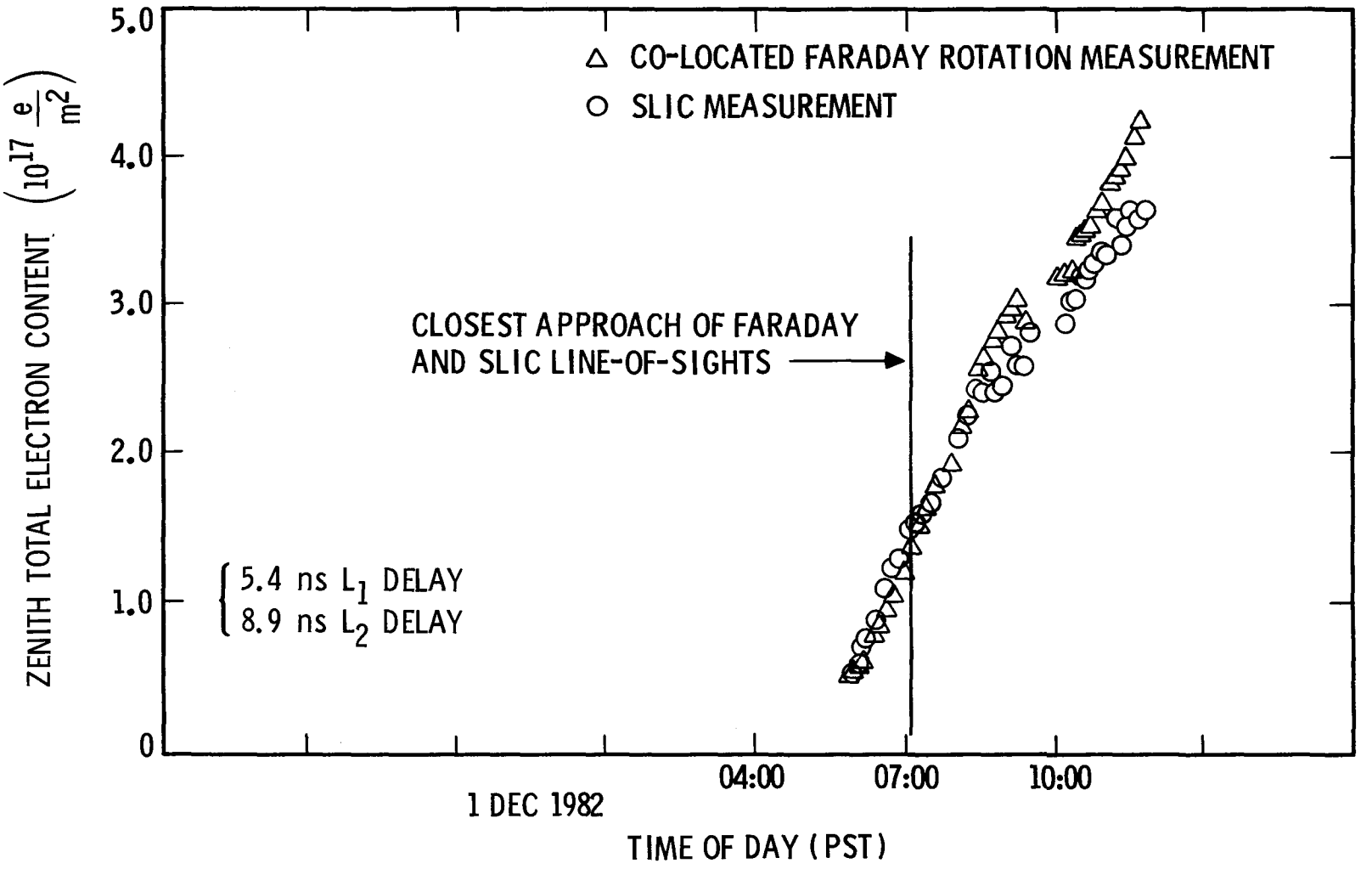

Figure 13. The SERIES ionospheric measurements are shown as circles, while the Faraday rotation results are triangles. The rapidly increasing TEC is due to the fact that the data were taken during sunrise. It can be seen that the agreement is better when the lines of sight for the two techniques are close, as this allows mapping errors to cancel.

G. 171 KM BASELINE

The 171 km baseline tests are sensitive to ephemeris errors (Fig. 14). Tropospheric delay corrections were applied to the baseline solution based on surface weather data (temperature, pressure and relative humidity) taken during the experiments. Ionospheric delay or SLIC corrections have been derived from the dual band SERIES data and applied. On the 171 km baseline between JPL and Goldstone, the error contribution due to a 10-meter uncertainty in the satellite ephemerides is estimated to be 9 cm.

The RMS scatter of the baseline lengths was 7 cm for the 171 km baseline. This is consistent with the presence of 10-meter errors in the ephemerides supplied by the NSWC.

H. BASELINE SUMMARY

A summary of the SERIES baseline testing results is given in Fig 15. This table represents the precision of the SERIES baseline measurement by the RMS scatter of the individual day's solutions. Typically, there were 12 days of data for each baseline. The accuracies of the SERIES measurements are shown through comparison with independent surveys.

I. BASELINE ERROR VS BASELINE LENGTH

Figure 14 shows the calculated effect of various error sources on baseline length determination accuracy for the current SERIES proof-of-concept system vs baseline length. For the shorter baselines, the SNR is the dominating error source. The errors due to both the SNR and clock terms can be reduced to less than 1-cm by more efficient data collection combined with more nearly simultaneous observations of the set of GPS satellites. The error shown for water vapor is based on the use of surface data to correct delays, and could be reduced with the use of current water vapor radiometers (WVR's). The ephemeris errors dominate for long baselines. The approach proposed by the JPL GPS development team to reduce ephemeris errors is to use a set of sites with positions determined by VLBI as fiducial points for a network of GPS receiver stations. Those observations made from the fiducial points would be used to obtain accurate ephemerides of the GPS satellites during each experiment.

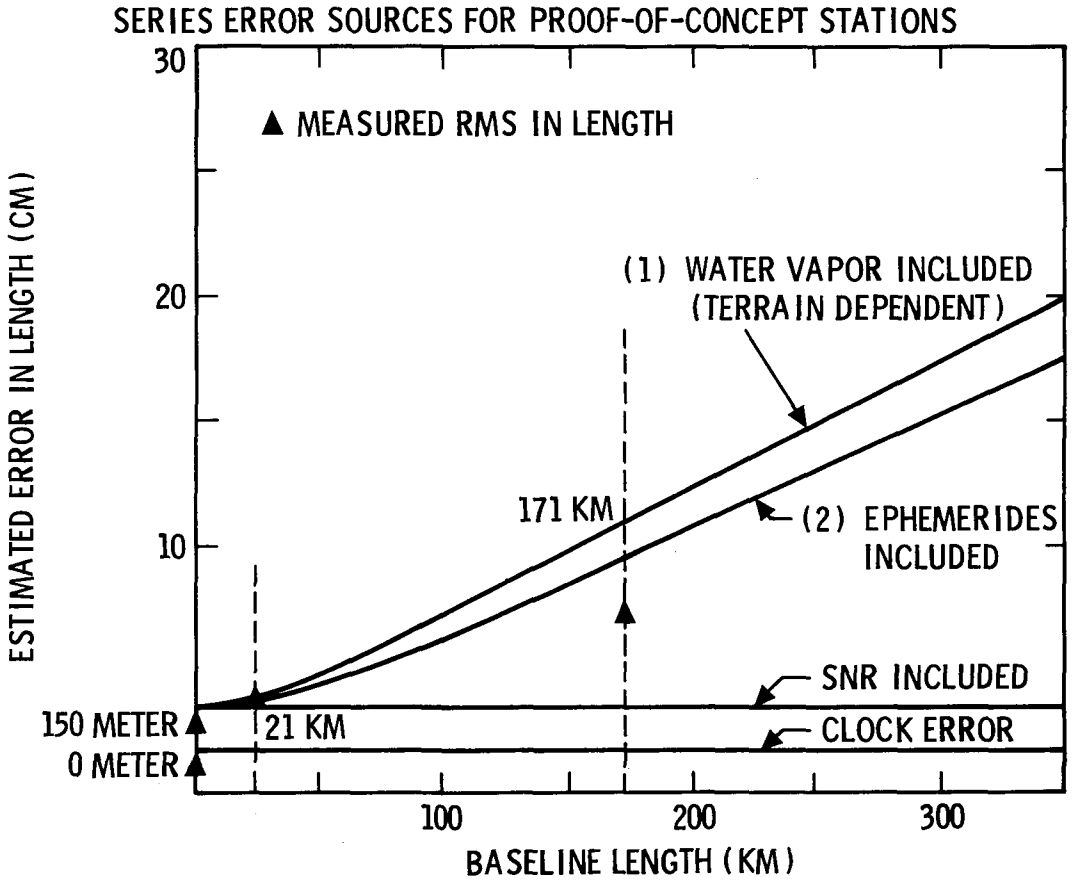

(1) SURFACE MODEL
(2) POST FIT EPHEMERIDES SUPPLIED BY NSWC (± 10 M ACCURACY ASSUMED)

Figure 14. The calculated cumulative error in baseline length is shown for the SERIES receivers as tested. It can be seen that for baselines longer than a few tens of km, the error is dominated by ephemeris and tropospheric calibration errors. The performance of the SERIES system is shown by the triangles for the 0, 150 m, 21 km, and 171 km baselines.

BASELINE LENGTH	RMS SCATTER IN LENGTH	DIFFERENCE OF MEAN LENGTH FROM SURVEY
0	1 CM	* +5 CM
150 M	3 CM	+0.3 CM
21 KM	4 CM	+ 1.2 CM
171 KM	7 CM	** + 7 CM, -1 CM

*ELECTRONIC CROSSTALK WAS THOUGHT TO CAUSE LENGTH BIAS

**DIFFERENCE FROM ARIES VLBI AND PRELIMINARY TEXAS LASER RESULTS RESPECTIVELY

Figure 15. Table of SERIES baseline results. Between 9 and 12 measurements were made at each of the baselines.

IX. CURRENT SERIES STATUS

The results of the tests described in the previous section show that the dominant error sources included primarily system noise and clock jitter on the short baselines (see Fig. 14). On the long baselines, orbit errors and the delays due to the presence of water vapor become important. Since the delays due to the ionosphere are measured in the SERIES receiver, these delays are calibrated.

As described previously, the errors due to water vapor delays can be reduced by the use of water vapor radiometers which measure those delays, and a network of high precision GPS receivers operating at known sites (fiducial stations) can be used to greatly reduce the orbital errors.

Improvements have already been made to the SERIES hardware and observation strategy, since taking the data contained in this report, to reduce the errors due to system noise and clock jitter. The clock errors were reduced by changing the time between satellite observations from two minutes to one minute. Three approaches have been used to reduce the error due to system noise.

The first of these was the reduction of the bandpass width of the P-code tracking filter. This allowed the data sampling to be closer to the desired Nyquist rate. The SERIES data sampling rate is currently limited by hardware constraints to ten samples per second. The bandwidth of the sampled signal was originally 80 Hz, and therefore had a Nyquist rate of 160 samples per second. The bandwidth is currently 20 Hz, with a Nyquist rate of 40 samples per second. The loss of SNR due to undersampling the P-code signal has been reduced to 0.25 from 0.0625.

The second approach was to replace the Bipolar Transistor preamplifier with a Gallium ArSenide Field Effect Transistor (GASFET) preamplifier. The table below shows the SERIES system temperatures, including the antenna temperature, for either preamplifier, at each of the two frequencies received.

Preamplifier	L_2 at 1227.6 MHZ	L_1 at 1575.42 MHZ
Bipolar Transistor	485 K	560 K
GASFET	95 K	125 K

The third approach to reduce the effect of system noise on pseudo range measurement accuracy was to acquire carrier range data. The capability to obtain carrier data from the L_2 frequency band has been added to the SERIES system. The advantage of carrier range data over P-code ranges is due to the fact that the recovered (squared) carrier wavelength is, for the L_2 carrier, 120 times shorter than the P-code "wavelength," and the error due to system noise is proportional to the wavelength. Therefore, for a given SNR on the L_2 band, the carrier range error due to system noise is 120 times less than the P-code range error due to system noise.

A potential problem with the use of the carrier range data type is the necessity to determine the pseudo-range ambiguity, equal to the wavelength of the squared carrier (12.1 cm for L_2). The capability to determine this ambiguity using the P-code pseudo-range measurement is predicted from current P-code performance, but has not, as yet, been tested experimentally.

Due to the high SNR resulting from the SERIES high gain antenna, the addition of the carrier data type to the already precise P-code data will make the SERIES receivers a unique tool. Potential uses, in addition to geodesy, are investigations of inherent limiting error sources of the space segment of the GPS, such as the possible presence of multipathing in the GPS satellite antennas. With or without the addition of the carrier range data type, the SERIES geodetic instrument has been demonstrated to be a GPS receiver capable of making accurate, cost effective measurements of baselines from sites located in remote areas.

X. SYMBOL GLOSSARY

$\vec{R}_u$	User/observer geocentric vector
$\vec{\rho}_s$	Satellite geocentric vector
ρ	Range from observer to satellite
ρ'	Measured pseudo range; $\rho' = \rho + c\ (\Delta t_u - \Delta t_s) + \text{noise}$
$\Delta\rho$	Differential pseudo range
$\Delta\rho'$	Measured differential pseudo range
$\Delta t = (t_u - t_s)$	Apparent delay in arrival of satellite clock pulses
Δt_u, Δt_s	User or satellite clock offset with respect to UTC (Universal Time Coordinated)
Δt_{si}	Clock offset of i^{th} satellite
δ	Correction term for converting spherical to planar wave fronts
$\hat{S}$	Unit vector from primary station to satellite signal source at distance ρ_i
$\vec{B}$	Baseline vector from remote station to primary station
t_{TM}	Time delay through transmission media
c	Speed of light
f	Code frequency in satellite reference frame
f_m	Code frequency measured by the user
$(\Delta tu_1 - \Delta tu_2)$	Clock offset of clock 2 relative to clock 1
N_i	P code or C/A code cycle ambiguity encountered at the i^{th} station
v_s	Satellite velocity
N	Integer number of whole wavelength cycles
$c/f = \lambda$	Effective wavelength of code at frequency f
f_i	Frequency measured at i^{th} station
T_i	Time of reception tagged by the TIC (Time Interval Counter)
$\theta_i = f_i T_i$	Fractional phase of the C/A or P codes
f_M	Measured Doppler frequency
ρ'_D	Measured Doppler pseudo range
t_g	Group delay effect; ionospheric time delay in seconds
I	Columnar electron content

T_g	Differential ionospheric group delay between L_1 and L_2 channels
C/A code	Coarse acquisition code with 1.023 MHz bit clocking rate, normally present in L_1 GPS band
P-code	Precision code with 10.23 MHz bit clocking rate, present in L_1 and L_2 GPS bands
L_1	GPS frequency band centered at 1.57542 GHz
L_2	GPS frequency band centered at 1.2276 GHz

REFERENCES

1. MacDoran, P. F., Spitzmesser, D. J., Buennagel, L. A., "SERIES: Satellite Emission Range Inferred Earth Surveying," Proceedings of the Third International Geodetic Symposium on Satellite Positioning, Las Cruces, New Mexico, Feb., 1982.

2. MacDoran, P. F., "Satellite Emission Radio Interferometric Earth Surveying, SERIES-GPS Geodetic System," Bulletin Geodesique, 53 (1979), pp. 117-138.

3. Young, L. E., Spitzmesser, D. J., Buennagel, L. A., "SERIES, A Novel Use of GPS Satellites for Positioning," Proceedings of the IAG/IUGG Symposium on Point Positioning in Marine Geodesy, Maracaibo, Feb., 1983.

4. Royden, H. N., Miller, R. B., Buennagel, L. B., "Comparison of NAVSTAR Satellite L-band Ionospheric Calibrations with Faraday-Rotation Measurements," to be published in Radio Science, May-June, 1984.

5. Buennagel, L. A., Spitzmesser, D. J., and Young, L. E., Proceedings of the Fourteenth Annual Precise Time and Time Interval (PTTI) application and Planning Meeting, Dec., 1982.

6. Spilker, J. J., Jr., "GPS Signal Structure and Performance Characteristics," Navigation Vol. 25, 121-146 (1978).

7. Milliken, R. J., and Zoller, C. J., "Principle of Operation of NAVSTAR and System Characteristics," Navigation Vol. 25, Summer, 1978

8. Ong, K. M., MacDoran, P. F., "Quasars and Artificial Satellites for Geodynamics Monitoring and Earthquake Research," International Conference on Cybernetics and Society, October, 1979.

9. Spiker, J. J., Jr., Digital Communications by Satellite, Prentice-Hall, Inc., Englewood Cliffs, New Jersey, 1977.

10. Viterbi, A. J., Principles of Coherent Communications, McGraw-Hill, 1966.

11. Bartholomew, C. A., "Satellite Frequency Standards," Navigation, Vol. 25, Summer, 1978.

12. Thomas, J. B., "An Analysis of Long Baseline Radio Interferometry," The Deep Space Network Progress Report, Tech. Rep. 32-1526, Vol. 7, p. 37, Jet Propulsion Laboratory, Pasadena, California, 1972a.

13. Niell, A. E., K. M. Ong, P. F. MacDoran, G. M. Resch, D. W. Fite, L. J. Skjerve, D. J. Spitzmesser, D. D. Morabito, L. Tanida, E. S. Claflin, B. B. Johnson, M. G. Newsted, A. Banisch, and J. F. Dracup: "Comparison of a Radio Interferometric Differential Baseline Measurement with Conventional Geodesy," Tectonophysics, 52, p. 532, 1979.

14. Russell, S. S., Schaibly, J. H., "Control Segment and User Performance," Navigation, Vol. 25, Summer, 1978.

15. MacDoran, P. F., SERIES-Satellite Emission Radio Interferometric Earth Surveying, Third Annual NASA Geodynamics Program Review, Crustal Dynamics Project Geodynamics Research, NASA, Washington, D.C., pp. 76 (1981).

16. Koehler, R. L., "Radio Propagation Measurements of Pulsed Plasma Streams From the Sun Using Pioneer Spacecraft," J. Geophysical Research 73, 115, 4483-4894 (1968).

17. Interface Control Document, 03953, Space Division, Rockwell International Corporation, September, 1975.

NASA—JPL—Coml., L.A., Calif.